Dynamic positioning of an uninhabited surface vehicle using state-dependent Riccati equation and pseudospectral method

Haibin Huang[a,b], Sanjay Sharma[b], Yufei Zhuang[a,b] and Dianguo Xu[c]

[a] Harbin Institute of Technology, Weihai, PR China
[b] Plymouth University, Plymouth, United Kingdom
[c] Harbin Institute of Technology, Harbin, PR China

Abstract: This paper proposed a novel control method for dynamic positioning of an uninhabited surface vehicle (USV). A state-dependent Riccati equation (SDRE) technique was introduced to deal with dynamic positioning problem of the USV. A new state-dependent coefficient (SDC) matrix was built to show the relationship between variables and satisfy the control inputs saturation for practical application. In order to solve the SDRE in real time, a semi-analytical formulation was derived by using Legendre-Gauss-Radau pseudospectral method. Simulation results show that the proposed method can be applied in real time and the USV can maintain its position and heading accurately and remains stable.

Keywords: Uninhabited surface vehicle, Dynamic positioning, State-dependent Riccati equation, Pseudospectral method

1. Introduction

The application of USV has gained a growing interest in recent years. Dynamic positioning (DP) is one of the important parts for USV, which might be defined as a system automatically controls a vessel to maintain its position and heading exclusively by means of active thrusters. There are many literatures about dynamic positioning. Here, only control methods for DP are reviewed, other literatures related about observer, control allocation, fault-tolerant or others can be seen in Sørensen (2011).

Sørensen *et al*. (1996) proposed a model-based control method where a feedforward

controller based on reference model was used to provide appropriate reference trajectories. A LQG controller was then used to minimize the thruster force and moment and the position error. Katebi *et al*. (1997) proposed a H∞ robust controller for DP system and weighting functions were presented to undertake the trade-off between track keeping and station keeping for a linear system. To avoid using linearization assumption for DP systems, Fossen and Grøvlen (1998) proposed a globally exponentially stable (GES) nonlinear control law using backstepping observer. However the environmental disturbances were neglected in this paper. Loria *et al*. (2000) considered the environmental disturbances and presented a similar globally asymptotically stabilizing (GAS) controller for DP using only position measurements. The stability proof was based on a separation principle which holds for the nonlinear ship model. The simulation results of two model ships *CyberShip I* and *CyberShip II* with different disturbances proved the stabilization of this method. Pettersen and Fossen (2000) proposed a time-varying feedback control law including integral action for DP of an underactuated ship. The proposed method was able to asymptotically stabilize the ship, providing exponential convergence to the desired position and orientation. The disturbances were not considered in this method and the simulation results showed oscillation and station error in case of disturbance. Nguyen *et al*. (2007) developed a hybrid controller for DP system in varying environmental conditions from calm to extreme seas. This hybrid controller contained multi-output PID and acceleration feedback controllers with position and acceleration measurements. Supervisory control was also used to switch the controller by considering the sea conditions. Tannuri *et al*. (2010) proposed a sliding mode control (SMC) method for DP system. A saturation function was used to eliminate the chattering that appears in the SMC. This controller was robust and easily tuned compared to PID controller. Muhammad and Doria-Cerezo (2012) proposed a passivity-based control method. The vessel model was rewritten as a port-Hamiltonian description, then an interconnection and damping assignment-passivity-based control (IDA-PBC) method based on port-Hamiltonian framework was presented. In this case only time invariable disturbance was considered for stability purpose. A similar method was proposed by Donaire and Perez (2012). The vessel model was also rewritten as an input-state-output port-Hamiltonian system (ISO-PHS), and then an integral action was used by considering a combination of passive and non-passive variables. This method also can be asymptotic stable with the constant disturbance and the states are bounded for any bounded disturbance. Du *et al*. (2013) proposed neural controller using the vectorial backstepping technique for DP. This

method didn't require any *priori* knowledge of the dynamics of the vessel and disturbances.

Most of the papers about DP system found in literatures are not designed for USV. It is more difficult to design the DP control system for USV than regular vessel as the disturbances would significantly affect the motion of the USV. Pereira *et al*. (2008) presented a weighted controller for station keeping of a small twin-propeller USV. This USV was underactuated, and wind was considered as the only disturbance. The control method weighted the line-of-sight controller and the disturbance. The ASV control was then designed to hold the vessel at a given place with the heading against the direction of wind. Panagou and Kyriakopoulos (2014) presented a state feedback control solution for the navigation and practical stabilisation of an underactuated marine vehicle under non-vanishing current disturbances. The control scheme consisted of three control laws. The first one was based on a novel dipolar vector field and was active when vehicle went out of the goal set to bring it back within the set. The other two control laws were active within the goal set and alternately regulate the position and the orientation of the vehicle and the system was practically stable around the desired position.

Most of the papers above considered only simple disturbances and cannot be applied to the USV working in real sea. This paper introduces a novel method to solve complex state-dependent Riccati equation (SDRE) in an efficient way to make the dynamic positioning viable in real time in harsh environmental conditions. The solution of SDRE is the optimal control inputs for dynamic positioning, and a Legendre-Gauss-Radau pseudospectral method is used to derive the semi-analytical formulation for SDRE so that this method can be used in real-time for practical applications.

The rest of this paper is organised as follows: Section 2 introduces the mathematical equations representing the motion of an USV. Section 3 describes the principle of SDRE, and the method to deal with control inputs saturation using SDRE. Section 4 proposes a method to solve SDRE problem using Legendre-Gauss-Radau (LGR) pseudospectral method. Section 5 shows the simulation results of the proposed algorithm and section 6 provides the conclusions.

2. Mathematical representation

Two types of reference frames are defined in this paper to describe the six degrees of freedom (6DOF) for an USV as shown in Fig. 1. The earth-fixed frame is fixed to the earth, with the X-axis points towards the North, the Y-axis points towards the East, and the Z-axis points towards the centre of the Earth. The body-fixed frame is fixed to the USV, with the x_b-axis points towards the bow, the y_b-axis points towards the starboard,

and the z_b-axis points downwards.

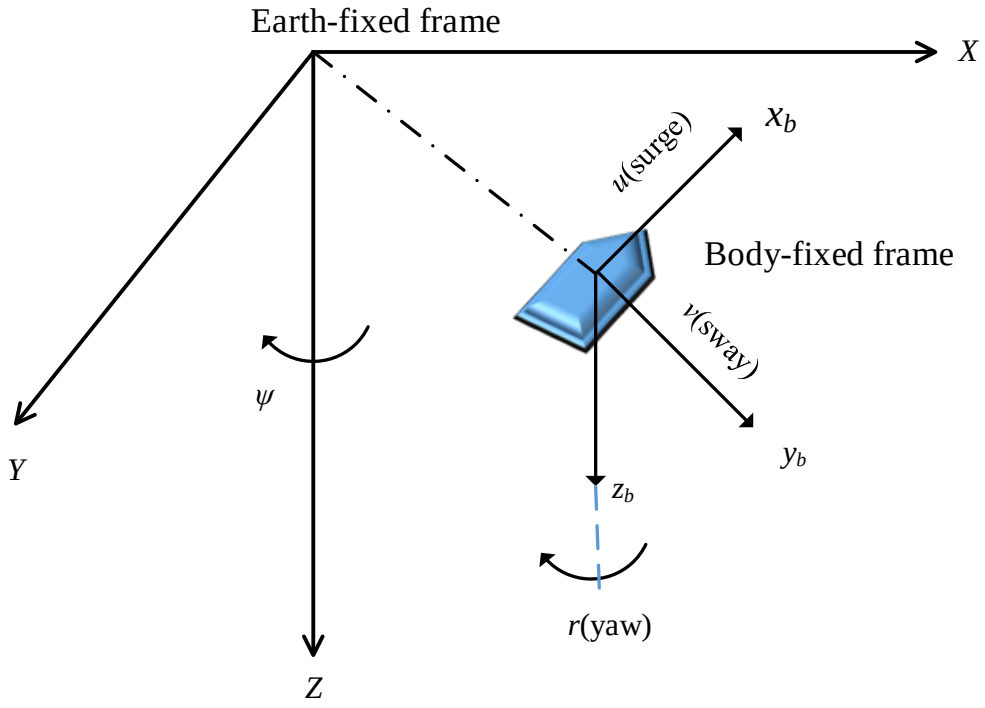

Fig. 1. Definition of the Earth-fixed and body-fixed frames

In this study, it is assumed that the center of buoyancy and the center of mass are the same, and the motion of heave, pitch and roll are negligible. The nonlinear equations of motion for an USV thus can be written as (Fossen, 1994):

$$\dot{\boldsymbol{\eta}} = \boldsymbol{R}(\psi)\boldsymbol{v} \tag{1}$$

$$\boldsymbol{M}\dot{\boldsymbol{v}} + \boldsymbol{C}(\boldsymbol{v})\boldsymbol{v} + \boldsymbol{D}(\boldsymbol{v})\boldsymbol{v} = \boldsymbol{f} + \boldsymbol{f}_{\text{Env}} \tag{2}$$

Here, $\boldsymbol{\eta}=[x, y, \psi]^{\text{T}}$ denotes the position and orientation vector with coordinates in the earth-fixed frame, $\boldsymbol{v}=[u, v, r]^{\text{T}}$ denotes the linear and angular velocity vector with coordinates in the body-fixed frame. $\boldsymbol{R}(\psi)$ is the translation matrix defined as:

$$\boldsymbol{R}(\psi) = \begin{bmatrix} \cos\psi & -\sin\psi & 0 \\ \sin\psi & \cos\psi & 0 \\ 0 & 0 & 1 \end{bmatrix} \tag{3}$$

$\boldsymbol{M}$ is the system inertia matrix including added mass, $\boldsymbol{C}(\boldsymbol{v})$ is the matrix of Coriolis and centripetal matrix of the rigid-body, $\boldsymbol{D}(\boldsymbol{v})$ is damping matrix, $\boldsymbol{f}$ is the vector of control inputs and $\boldsymbol{f}_{\text{Env}}$ is the environmental force and moments acting on the vessel. These matrixes can also be decomposed as follows:

$$\boldsymbol{M} = \boldsymbol{M}_{RB} + \boldsymbol{M}_A = \begin{bmatrix} m - X_{\dot{u}} & 0 & 0 \\ 0 & m - Y_{\dot{v}} & 0 \\ 0 & 0 & I_z - N_{\dot{r}} \end{bmatrix} \tag{4}$$

where m and I_z are the mass and moment of inertia of USV respectively, $X_{\dot{u}}$, $Y_{\dot{v}}$ and $N_{\dot{r}}$ are the parameters for added mass effects.

$$\boldsymbol{C}(\boldsymbol{v}) = \boldsymbol{C}_{RB}(\boldsymbol{v}) + \boldsymbol{C}_A(\boldsymbol{v}) \tag{5}$$

$$\boldsymbol{C}_{RB}(\boldsymbol{v}) = \begin{bmatrix} 0 & 0 & -m(x_G r + v) \\ 0 & 0 & mu \\ m(x_G r + v) & -mu & 0 \end{bmatrix} \tag{6}$$

$$\boldsymbol{C}_A(\boldsymbol{v}) = \begin{bmatrix} 0 & 0 & Y_{\dot{v}} v + Y_{\dot{r}} r \\ 0 & 0 & -X_{\dot{u}} u \\ -Y_{\dot{v}} v - Y_{\dot{r}} r & X_{\dot{u}} u & 0 \end{bmatrix} \tag{7}$$

where $\boldsymbol{C}_{RB}$ is the Coriolis and centripetal matrix of the rigid-body, $\boldsymbol{C}_A$ is the hydrodynamic Coriolis and centripetal matrix.

For a low speed USV, the nonlinear damping can be neglected, and only linear damping will be considered here. The matrix $\boldsymbol{D}$ is given by:

$$\boldsymbol{D} = \begin{bmatrix} -X_u & 0 & 0 \\ 0 & -Y_v & -Y_r \\ 0 & -N_v & -N_r \end{bmatrix} \tag{8}$$

$$\boldsymbol{f}_{Env} = \boldsymbol{f}_{\text{wind}} + \boldsymbol{f}_{\text{wave}} + \boldsymbol{f}_{\text{current}} + \boldsymbol{f}_{\text{other}} \tag{9}$$

where, $\boldsymbol{f}_{\text{wind}}$ and $\boldsymbol{f}_{\text{current}}$ are the disturbance force and moment caused by wind, wave and current, $\boldsymbol{f}_{\text{other}}$ is the force and moment caused by other random disturbances.

3. State-dependent Riccati equation

3.1. Problem Formulation

Consider a nonlinear time-varying system in the form

$$\dot{\boldsymbol{x}}(t) = \boldsymbol{f}(\boldsymbol{x}, t) + \boldsymbol{g}(\boldsymbol{x}, \boldsymbol{u}, t) \tag{10}$$

where $\boldsymbol{x} = [x_1, x_2, \cdots, x_n]^T \in \mathbb{R}^n$ is the state vector, and $\boldsymbol{u} = [u_1, u_2, \cdots, u_m]^T \in \mathbb{R}^m$ is the control input vector for each $t \in \mathbb{R}^+$, $\boldsymbol{f}$ and $\boldsymbol{g}$ are continuous functions of $\boldsymbol{x}$, and $\boldsymbol{f}(\boldsymbol{0}, t) = \boldsymbol{0}$ is an equilibrium point with $\boldsymbol{u} = \boldsymbol{0}$. This nonlinear system can be converted into a linear form as:

$$\dot{\boldsymbol{x}}(t) = \boldsymbol{A}(\boldsymbol{x})\boldsymbol{x}(t) + \boldsymbol{B}(\boldsymbol{x})\boldsymbol{u}(t) \tag{11}$$

which is also called state-dependent coefficient (SDC) parameterization formulation. Here $\boldsymbol{f}(\boldsymbol{x}) = \boldsymbol{A}(\boldsymbol{x})\boldsymbol{x}(t)$ and $\boldsymbol{g}(\boldsymbol{x},\boldsymbol{u},t) = \boldsymbol{B}(\boldsymbol{x})\boldsymbol{u}(t)$ (Çimen, 2010). SDRE method is a state feedback control law to minimize the quadratic-like performance index

$$J = \frac{1}{2}\int_0^\infty \{\boldsymbol{x}^T(t)\boldsymbol{Q}(\boldsymbol{x})\boldsymbol{x}(t) + \boldsymbol{u}^T(t)\boldsymbol{R}(\boldsymbol{x})\boldsymbol{u}(t)\}\mathrm{d}t \tag{12}$$

where $\boldsymbol{Q}$ is the symmetric positive semi-definite weighting matric for states, and $\boldsymbol{R}$ is the symmetric positive definite weighting matric for inputs.

It can be seen that the SDC parameterization formulation and its performance index is similar with linear quadratic regulator (LQR). The solution of this infinite time horizon nonlinear optimal control (ITHNOC) problem is also inspired by LQR. For $\forall \boldsymbol{x} = \boldsymbol{\Omega}$, if the pair $\{\boldsymbol{A}(\boldsymbol{x}), \boldsymbol{B}(\boldsymbol{x})\}$ is pointwise stabilizable, and the pair $\{\boldsymbol{A}(\boldsymbol{x}), \boldsymbol{C}(\boldsymbol{x})\}$ is pointwise detectable, where $\boldsymbol{C}^T(\boldsymbol{x})\boldsymbol{C}(\boldsymbol{x}) = \boldsymbol{Q}(\boldsymbol{x})$, then the optimal control for eqn. (11), (12) is (Cloutier, 1997):

$$\boldsymbol{U}(\boldsymbol{x}) = -\boldsymbol{R}^{-1}(\boldsymbol{x})\boldsymbol{B}(\boldsymbol{x})\boldsymbol{P}(\boldsymbol{x})\boldsymbol{x} \tag{13}$$

where $\boldsymbol{P}(\boldsymbol{x})$ is the unique, symmetric nonnegative definite solution of the algebraic SDRE

$$\boldsymbol{P}(\boldsymbol{x})\boldsymbol{A}(\boldsymbol{x}) + \boldsymbol{A}^T(\boldsymbol{x})\boldsymbol{P}(\boldsymbol{x}) - \boldsymbol{P}(\boldsymbol{x})\boldsymbol{B}(\boldsymbol{x})\boldsymbol{R}^{-1}(\boldsymbol{x})\boldsymbol{B}^T(\boldsymbol{x})\boldsymbol{P}(\boldsymbol{x}) + \boldsymbol{Q}(\boldsymbol{x}) = \boldsymbol{0} \tag{14}$$

3.2. The choice of SDC matrix

Let $x_G = 0$, and $Y_{\dot{r}}$=0, then Eqn. (1) and (2) can be rewritten as

$$\begin{aligned}
\begin{bmatrix} \dot{x} \\ \dot{y} \\ \dot{\psi} \\ \dot{u} \\ \dot{v} \\ \dot{r} \end{bmatrix} &= \begin{bmatrix} 0 & 0 & 0 & \cos\psi & -\sin\psi & 0 \\ 0 & 0 & 0 & \sin\psi & \cos\psi & 0 \\ 0 & 0 & 0 & 0 & 0 & 1 \\ 0 & 0 & 0 & -d_{11}/m_{11} & 0 & -c_{13}v/m_{11} \\ 0 & 0 & 0 & 0 & -d_{22}/m_{22} & -c_{23}u - d_{23}/m_{22} \\ 0 & 0 & 0 & -c_{31}v/m_{33} & -c_{32}u - d_{32}/m_{33} & -d_{33}/m_{33} \end{bmatrix} \begin{bmatrix} x \\ y \\ \psi \\ u \\ v \\ r \end{bmatrix} + \\
&\quad \begin{bmatrix} 0 & 0 & 0 \\ 0 & 0 & 0 \\ 0 & 0 & 0 \\ 1/m_{11} & 0 & 0 \\ 0 & 1/m_{22} & 0 \\ 0 & 0 & 1/m_{33} \end{bmatrix} \begin{bmatrix} f_u \\ f_v \\ f_\psi \end{bmatrix} \\
&= \tilde{\boldsymbol{A}}(\boldsymbol{x})\boldsymbol{x} + \tilde{\boldsymbol{B}}(\boldsymbol{x})\boldsymbol{u}
\end{aligned} \tag{15}$$

where $m_{11} = m - X_{\dot{u}}$, $m_{22} = m - Y_{\dot{v}}$, $m_{33} = I_z - N_{\dot{r}}$, $c_{13} = (-m + Y_{\dot{v}})v$, $c_{23} = (m - X_{\dot{u}})u$, $c_{31} = (m - Y_{\dot{v}})v$, $c_{32} = (-m + X_{\dot{u}})u$, $d_{11} = -X_u$, $d_{22} = -Y_v$, $d_{23} = -Y_r$, $d_{32} = -N_v$, $d_{33} = -N_r$.

Obviously, if $\boldsymbol{A}(\boldsymbol{x})=\tilde{\boldsymbol{A}}(\boldsymbol{x})$ and $\boldsymbol{B}(\boldsymbol{x})=\tilde{\boldsymbol{B}}(\boldsymbol{x})$, and the pairs $\{\tilde{\boldsymbol{A}}(\boldsymbol{x}),\ \tilde{\boldsymbol{B}}(\boldsymbol{x})\}$ $\{\tilde{\boldsymbol{A}}(\boldsymbol{x}),\ \boldsymbol{C}(\boldsymbol{x})\}$ is pointwise stabilizable and pointwise detectable for $\forall \boldsymbol{x}=\boldsymbol{\Omega}$, then the optimal control inputs can be obtained by Eqn. (13) and (14). There are many other ways to build a SDC matrix for a multivariable nonlinear system, i.e. the SDC matrix $\boldsymbol{A}(\boldsymbol{x})$ is not unique. According to Çimen (2012), the SDC matrix $\boldsymbol{A}(\boldsymbol{x})$ should reflect the relationship of respective variables, and $\tilde{\boldsymbol{A}}(\boldsymbol{x})$ does not satisfy this requirement. For example, $\tilde{A}(1,3)=0$ doesn't tell the relationship between ψ, u and v. To deal with this problem, a new $\boldsymbol{A}(\boldsymbol{x})$ is defined as follows:

$$\boldsymbol{A}(\boldsymbol{x})=\begin{bmatrix}
0 & 0 & \alpha_{x1}\dfrac{\cos\psi-1}{\psi}u-\alpha_{x2}\dfrac{\sin\psi}{\psi}v & (1-\alpha_{x1})(\cos\psi-1)+1 & -(1-\alpha_{x2})\sin\psi & 0\\
0 & 0 & \alpha_{y1}\dfrac{\sin\psi}{\psi}u+\alpha_{y2}\dfrac{\cos\psi-1}{\psi}v & (1-\alpha_{y1})\sin\psi & (1-\alpha_{y2})(\cos\psi-1)+1 & 0\\
0 & 0 & 0 & 0 & 0 & 1\\
0 & 0 & 0 & -\dfrac{d_{11}}{m_{11}} & -\dfrac{c_{13}}{m_{11}}\alpha_u r & -\dfrac{c_{13}}{m_{11}}(1-\alpha_u)v\\
0 & 0 & 0 & -\dfrac{c_{23}}{m_{22}}\alpha_v r & -\dfrac{d_{22}}{m_{22}} & -\dfrac{c_{23}}{m_{22}}(1-\alpha_v)u-\dfrac{d_{23}}{m_{22}}\\
0 & 0 & 0 & \dfrac{c_{31}-c_{32}}{m_{33}}\alpha_r v-\dfrac{c_{31}}{m_{33}}v & \dfrac{c_{32}-c_{31}}{m_{33}}\alpha_r u-\dfrac{c_{32}}{m_{33}}u-\dfrac{d_{32}}{m_{33}} & -\dfrac{d_{33}}{m_{33}}
\end{bmatrix} \tag{16}$$

here, $\boldsymbol{\alpha}=\begin{bmatrix}\alpha_{x1} & \alpha_{x2} & \alpha_{y1} & \alpha_{y2} & \alpha_{\psi} & \alpha_u & \alpha_v & \alpha_r\end{bmatrix}^T$ can be chosen between 0 and 1, and $\boldsymbol{A}(\boldsymbol{x})=\tilde{\boldsymbol{A}}(\boldsymbol{x})$ when $\boldsymbol{\alpha}=\boldsymbol{0}^{8\times1}$. In this way the new SDC matrix $\boldsymbol{A}(\boldsymbol{x})$ can reflect the relationships of all the variables, and the choice of $\boldsymbol{\alpha}$ is flexible and can help enhance the performance index.

3.3. Control Input Saturation

For a practical USV, the control actuators are hard-bounded, so the control system might be unstable without considering the control input saturation. The control input vectors are assumed to use continuous force and moment confined to lie within specified limits

$$\left|\boldsymbol{f}(t)\right|\le \boldsymbol{f}_{\max} \tag{17}$$

where

$$\begin{aligned}\boldsymbol{f}&=\begin{bmatrix}f_u & f_v & f_\psi\end{bmatrix}^{\mathrm{T}}\\ \boldsymbol{f}_{\max}&=\begin{bmatrix}f_{u\max} & f_{v\max} & f_{\psi\max}\end{bmatrix}^{\mathrm{T}}\end{aligned} \tag{18}$$

For f_u, two new variables τ_u and f_{u1} are introduced, let (Mracek and Cloutier 1998)

$$f_u = \text{sat}\sin(f_{u\max}, \tau_u) \tag{19}$$

$$\text{sat}\sin(f_{u\max}, \tau_u) = \begin{cases} f_{u\max}, & \tau_u > \dfrac{\pi}{2} \\ f_{u\max}\sin(\tau_u), & -\dfrac{\pi}{2} \le \tau_u \le \dfrac{\pi}{2} \\ -f_{u\max}, & \tau_u < -\dfrac{\pi}{2} \end{cases} \tag{20}$$

and

$$\dot{\tau}_u = f_{u1} \tag{21}$$

The equations for f_v and f_ψ are straight forward

$$\begin{aligned} f_v &= \text{sat}\sin(f_{v\max}, \tau_v) & f_\psi &= \text{sat}\sin(f_{\psi\max}, \tau_\psi) \\ \dot{\tau}_v &= f_{v1} & \dot{\tau}_\psi &= f_{\psi 1} \end{aligned} \tag{22}$$

With this method, f_u, f_v and f_ψ will lay in the given interval no matter what f_{u1}, f_{v1} and $f_{\psi 1}$ will be.

Then Eqn(15) can be extended as:

$$\dot{\bar{\boldsymbol{x}}} = \bar{\boldsymbol{A}}(\bar{\boldsymbol{x}})\bar{\boldsymbol{x}} + \bar{\boldsymbol{B}}(\bar{\boldsymbol{x}})\bar{\boldsymbol{f}} \tag{23}$$

where

$$\bar{\boldsymbol{x}} = \begin{bmatrix} x & y & \psi & u & v & r & \tau_u & \tau_v & \tau_\psi \end{bmatrix}^{\mathrm{T}} \tag{24}$$

$$\bar{\boldsymbol{f}} = \begin{bmatrix} f_{u1} & f_{v1} & f_{\psi 1} \end{bmatrix}^{\mathrm{T}} \tag{25}$$

$$\bar{\boldsymbol{A}} = \begin{bmatrix} \boldsymbol{A}(\boldsymbol{x}) & \boldsymbol{E}(\boldsymbol{x}) \\ \boldsymbol{0}^{3\times 6} & \boldsymbol{0}^{3\times 3} \end{bmatrix} \tag{26}$$

$$\boldsymbol{E}(\boldsymbol{x}) = \begin{bmatrix} \boldsymbol{0}^{3\times 3} \\ \hline \dfrac{1}{m_{11}}\dfrac{\text{sat}\sin(f_{u\max}, \tau_u)}{\tau_u} & 0 & 0 \\ 0 & \dfrac{1}{m_{22}}\dfrac{\text{sat}\sin(f_{v\max}, \tau_v)}{\tau_v} & 0 \\ 0 & 0 & \dfrac{1}{m_{33}}\dfrac{\text{sat}\sin(f_{\psi\max}, \tau_\psi)}{\tau_\psi} \end{bmatrix} \tag{27}$$

$$\bar{\boldsymbol{B}} = \begin{bmatrix} \boldsymbol{0}^{6\times 3} \\ \hdashline \boldsymbol{I}^{3\times 3} \end{bmatrix} \tag{28}$$

The performance index Eqn. (12) is then derived as:

$$J = \frac{1}{2}\int_0^\infty \{\bar{\boldsymbol{x}}^{\mathrm{T}}\bar{\boldsymbol{Q}}\bar{\boldsymbol{x}} + \bar{\boldsymbol{f}}^{\mathrm{T}}\bar{\boldsymbol{R}}\bar{\boldsymbol{f}}\}\mathrm{d}t \tag{29}$$

and the optimal control inputs for Eqn. (23) should be written as

$$\bar{\boldsymbol{f}}(\bar{\boldsymbol{x}}) = -\bar{\boldsymbol{R}}^{-1}(\bar{\boldsymbol{x}})\bar{\boldsymbol{B}}\bar{\boldsymbol{P}}(\bar{\boldsymbol{x}})\bar{\boldsymbol{x}} \tag{30}$$

where $\bar{\boldsymbol{P}}(\bar{\boldsymbol{x}})$ is the solution of the new algebraic SDRE

$$\bar{\boldsymbol{P}}(\bar{\boldsymbol{x}})\bar{\boldsymbol{A}}(\bar{\boldsymbol{x}}) + \bar{\boldsymbol{A}}^{\mathrm{T}}(\bar{\boldsymbol{x}})\bar{\boldsymbol{P}}(\bar{\boldsymbol{x}}) - \bar{\boldsymbol{P}}(\bar{\boldsymbol{x}})\bar{\boldsymbol{B}}(\bar{\boldsymbol{x}})\bar{\boldsymbol{R}}^{-1}\bar{\boldsymbol{B}}^{T}(\bar{\boldsymbol{x}})\bar{\boldsymbol{P}}(\bar{\boldsymbol{x}}) + \bar{\boldsymbol{Q}}(\bar{\boldsymbol{x}}) = \boldsymbol{0} \tag{31}$$

Then the $\bar{\boldsymbol{x}}$ can be obtained, and the true control inputs $\boldsymbol{f}$ for the dynamic positioning of USV can be derived using Eqn. (19) and (22).

4. Solving SDRE using a pseudospectral method

The controller needs to solve the SDRE in real-time for the dynamic positioning mission, which can also be considered as solving a LQR in real-time. However the solution methods of LQR come with high computation cost and sometimes unstable. In this paper, a pseudospectral method is induced to solve the SDRE in real-time which is stable and will require less computational burden.

4.1. Legendre-Gauss-Radau pseudospectral method

Let $L_N(t)$ denote the Legendre polynomial of order N, and let t_i, $i = 1, 2, \cdots N$ be the zeros of $L_N(t)+L_{N+1}(t)$, with $t_0 = -1$. These N+1 points are called Legendre-Gauss-Radau (LGR) points. These LGR points are distributed over [-1,1), this kind of fixed at the left hand endpoint interval is quite suitable for the ITHNOC problem.

For a given function $F(t)$ defined at $[-1,1)$, it can be approximated by a Nth degree interpolation polynomial as (Fahroo and Ross, 2008)

$$F^N(t) \coloneqq \sum_{i=0}^{N} F(t_i)\phi_i(t) \tag{32}$$

where $\phi_i(t)$ satisfies the relationship $\phi_i(t_j) = \delta_{ij}$, and δ_{ij} is the Kronecker delta.

The integral of $F^N(t)$ is

$$\int_{-1}^{1} F^N(t)dt \coloneqq \sum_{i=0}^{N} F(t_i)w_i \tag{33}$$

where

$$w_i = \begin{cases} \dfrac{2}{(N+1)^2}, & i = 0 \\ \dfrac{1-t_i}{(N+1)^2[L_N(t_i)]^2}, & 1 \le i \le N \end{cases} \tag{34}$$

The derivative of $F^N(t)$ is

$$\dot{F}^N(t_i) = \sum_{j=0}^{N} D_{ij} F(t_j) \tag{35}$$

where $\boldsymbol{D} := (D_{ij})$ is an $(N+1)\times(N+1)$ matrix, given by

$$\boldsymbol{D} = (D_{ij}) := \begin{cases} -\dfrac{N(N+2)}{4} & i = j = 0 \\ \dfrac{L_N(t_i)}{L_N(t_j)} \dfrac{1-t_j}{1-t_i} \dfrac{1}{(t_i - t_j)} & i \neq j, 1 \le i, j \le N \\ \dfrac{1}{2(1-t_i)} & 1 \le i = j \le N \end{cases} \tag{36}$$

4.2. Solution Approach

As mentioned above, the LGR points should be in the interval [-1, 1), so that the original optimal problem should be restated from [0, +∞) to [-1, 1) with the transformation of the independent variable τ (Garg, Hager and Rao, 2011)

$$\tau = \ln\left(\frac{2}{1-t}\right), \quad t \in [0, +\infty) \tag{37}$$

and

$$\frac{dt}{d\tau} = \frac{1}{1-\tau} \tag{38}$$

At an arbitrary sample time t_0, the control inputs should be the solution of Eqn. (31) at t_0, or they can be considered as the solution of a LQR problem. Let the state equation

$$\dot{\bar{\boldsymbol{x}}}(t) = \bar{\boldsymbol{A}}(\bar{\boldsymbol{x}}(t_0))\bar{\boldsymbol{x}}(t) + \bar{\boldsymbol{B}}\bar{\boldsymbol{f}}(t) \tag{39}$$

with the co-state equation

$$\dot{\bar{\boldsymbol{\lambda}}}(t) = -\bar{\boldsymbol{Q}}\bar{\boldsymbol{x}}(t_0) - \bar{\boldsymbol{A}}(\bar{\boldsymbol{x}}(t_0))\bar{\boldsymbol{\lambda}}(t) \tag{40}$$

and the desired control inputs are

$$\bar{\boldsymbol{f}}(t_0) = -\bar{\boldsymbol{R}}^{-1}\bar{\boldsymbol{B}}\bar{\boldsymbol{P}}(t_0)\bar{\boldsymbol{x}}(t_0) = -\bar{\boldsymbol{R}}^{-1}\bar{\boldsymbol{B}}\bar{\boldsymbol{\lambda}}(t_0) \tag{41}$$

If $\bar{\boldsymbol{\lambda}}(t_0)$ can be solved in real-time, the entire SDRE problem for dynamic positioning of the USV can then be solved.

The $\bar{\boldsymbol{x}}(t)$ and $\bar{\boldsymbol{\lambda}}(t)$ can be approximated using ϕ

$$\bar{\boldsymbol{x}}(\tau) \approx \bar{\boldsymbol{x}}^N(\tau) = \sum_{j=0}^{N} \bar{\boldsymbol{x}}_j \phi_j(\tau) \tag{42}$$

$$\bar{\boldsymbol{\lambda}}(\tau) \approx \bar{\boldsymbol{\lambda}}^N(\tau) = \sum_{j=0}^{N} \bar{\boldsymbol{\lambda}}_j \phi_j(\tau) \tag{43}$$

and

$$\dot{\bar{\boldsymbol{x}}}_i(\tau) \approx \sum_{j=0}^{N} D_{ij} \bar{\boldsymbol{x}}_j, \ \ i = 0,1,\cdots N \tag{44}$$

$$\dot{\bar{\boldsymbol{\lambda}}}_i(\tau) \approx \sum_{j=0}^{N} D_{ij} \bar{\boldsymbol{\lambda}}_j, \ \ i = 0,1,\cdots N \tag{45}$$

So Eqn. (39) and (40) can be transferred as

$$\sum_{j=0}^{N} D_{ij} \bar{\boldsymbol{x}}_j - \frac{1}{1-\tau_i}(\bar{\boldsymbol{A}}_0 \bar{\boldsymbol{x}}_i - \bar{\boldsymbol{R}}^{-1} \bar{\boldsymbol{B}} \bar{\boldsymbol{\lambda}}_i) = \boldsymbol{0}^{9\times 1}, \quad i = 0,1,\cdots N \tag{46}$$

$$\sum_{j=0}^{N} D_{ij} \bar{\boldsymbol{\lambda}}_i + \frac{1}{1-\tau_i}(\bar{\boldsymbol{Q}} \bar{\boldsymbol{x}}_i + \bar{\boldsymbol{A}}_0 \bar{\boldsymbol{\lambda}}_i) = \boldsymbol{0}^{9\times 1}, \quad i = 0,1,\cdots N \tag{47}$$

Here, $\bar{\boldsymbol{A}}_0 = \bar{\boldsymbol{A}}(\bar{\boldsymbol{x}}(t_0))$. Let

$$\begin{aligned} \boldsymbol{X} &= [\bar{\boldsymbol{x}}_0^{\mathrm{T}} \quad \bar{\boldsymbol{x}}_1^{\mathrm{T}} \quad \cdots \quad \bar{\boldsymbol{x}}_N^{\mathrm{T}}]^{\mathrm{T}} \\ \boldsymbol{\Lambda} &= [\bar{\boldsymbol{\lambda}}_0^{\mathrm{T}} \quad \bar{\boldsymbol{\lambda}}_1^{\mathrm{T}} \quad \cdots \quad \bar{\boldsymbol{\lambda}}_N^{\mathrm{T}}]^{\mathrm{T}} \end{aligned} \tag{48}$$

Eqn. (46) and (47) can be written as (Yan, Fahroo and Ross, 2001)

$$\boldsymbol{V}\boldsymbol{Z} = \begin{bmatrix} \boldsymbol{V}_0 & \boldsymbol{V}_e \end{bmatrix} \begin{bmatrix} \boldsymbol{Z}_0 \\ \boldsymbol{Z}_e \end{bmatrix} = \boldsymbol{0}^{18(N+1)\times 1} \tag{49}$$

where $\boldsymbol{Z} = \begin{bmatrix} \boldsymbol{X}^{\mathrm{T}} & \boldsymbol{\Lambda}^{\mathrm{T}} \end{bmatrix}^{\mathrm{T}}$, $\boldsymbol{V}$ is a $18(N+1)\times 18(N+1)$ matrices which can be derived for eqn. (46) and (47). $\boldsymbol{V}_0$ is the first $18(N+1)\times 9$ block matrix of $\boldsymbol{V}$, and $\boldsymbol{V}_e$ is the rest of $\boldsymbol{V}$. $\boldsymbol{Z}_0 = \bar{\boldsymbol{x}}_0$, and $\boldsymbol{Z}_e = \begin{bmatrix} \bar{\boldsymbol{x}}_1^{\mathrm{T}} & \bar{\boldsymbol{x}}_2^{\mathrm{T}} & \cdots & \bar{\boldsymbol{x}}_N^{\mathrm{T}} & \bar{\boldsymbol{\lambda}}_0^{\mathrm{T}} & \bar{\boldsymbol{\lambda}}_1^{\mathrm{T}} & \cdots & \bar{\boldsymbol{\lambda}}_N^{\mathrm{T}} \end{bmatrix}^{\mathrm{T}}$ which can be derived as

$$\boldsymbol{Z}_e = -(\boldsymbol{V}_e \backslash \boldsymbol{V}_0)\boldsymbol{Z}_0 = \boldsymbol{W}\boldsymbol{Z}_0 \tag{50}$$

The '\' means the left matrix divide operator of Matlab. Then the following can be obtained:

$$\boldsymbol{Z} = \begin{bmatrix} \boldsymbol{X} \\ \boldsymbol{\Lambda} \end{bmatrix} = \begin{bmatrix} \boldsymbol{I}^{n\times n} \\ \boldsymbol{W} \end{bmatrix} \boldsymbol{Z}_0 = \begin{bmatrix} \boldsymbol{W}_x \\ \boldsymbol{W}_\lambda \end{bmatrix} \boldsymbol{Z}_0 \tag{51}$$

where $\boldsymbol{W}_x$ and $\boldsymbol{W}_\lambda$ are $9(N+1)\times 9$ matrices which can be obtained from $\begin{bmatrix} \boldsymbol{I}^{n\times n} & \boldsymbol{W} \end{bmatrix}^{\mathrm{T}}$.

thus

$$\boldsymbol{\Lambda}=\boldsymbol{W}_{\lambda}\boldsymbol{Z}_0$$
$$\begin{bmatrix}\bar{\boldsymbol{\lambda}}_0\\ \bar{\boldsymbol{\lambda}}_1\\ \vdots\\ \bar{\boldsymbol{\lambda}}_N\end{bmatrix}=\begin{bmatrix}\boldsymbol{W}_{\lambda 0}\\ \boldsymbol{W}_{\lambda 1}\\ \vdots\\ \boldsymbol{W}_{\lambda N}\end{bmatrix}\bar{\boldsymbol{x}}_0 \tag{52}$$

where $\bar{\boldsymbol{x}}_0=\bar{\boldsymbol{x}}(t_0)$, and the Eqn. (41) can be obtained by

$$\bar{\boldsymbol{f}}(t_0)=-\bar{\boldsymbol{R}}^{-1}\bar{\boldsymbol{B}}\bar{\boldsymbol{\lambda}}(t_0)=-\bar{\boldsymbol{R}}^{-1}\bar{\boldsymbol{B}}\boldsymbol{W}_{\lambda 0}\bar{\boldsymbol{x}}_0 \tag{53}$$

Now the control inputs are calculated by the following steps: i) Set $\begin{bmatrix}\tau_u & \tau_v & \tau_\psi\end{bmatrix}^{\mathrm{T}}=\boldsymbol{0}^{3\times 1}$ at the initial time. ii) At each sample time, get the current states $\bar{\boldsymbol{x}}(t_0)$, and then obtain $\bar{\boldsymbol{A}}_0$ using Eqn. (26). iii) Using Eqn. (46) and (47) derive $\boldsymbol{V}$. iv) Calculate $\boldsymbol{W}$ using Eqn. (50), and $\boldsymbol{W}_{\lambda 0}$ is a 9×9 block of $\boldsymbol{W}$. v) the control inputs can be obtained by using Eqn. (53). It can be seen that there are only one left matrix divide and some simple fundamental operations in this method, so it is simple enough to be calculated in real-time.

5. Simulation results

This work used the model of an USV at Plymouth University called *Springer*, which is approximately 4m long and 0.6 tones weight. The parameters of the fully actuated *Springer* USV as shown in Table 1 are used in this paper for simulation purpose.

Table 1
The constant parameters of the *Springer* USV

m, kg	600	X_u, N·s/m	-17.0
I_z, kg·m	550	Y_v, N·s/m	-29.2
$X_{\dot{u}}$, kg	-77.6	Y_r, N·s/m	-1
$Y_{\dot{v}}$, kg	-561.1	N_v, N·s/m	-1
$N_{\dot{r}}$, kg	-286.5	N_r, N·s/m	-19.8

5.1. The number of LGR points

The SDRE should be solved in real-time for practical applications. Different numbers of LGR points may have different effect on computational time and accuracy. Table 2 shows the results of different LGR points in 200s without considering any environment

disturbance. Control inputs saturation was not considered first, i.e. Eqn. (16) was used here with $\boldsymbol{Q}=10^6\times\boldsymbol{I}^{6\times6}$ and $\boldsymbol{R}=\boldsymbol{I}^{3\times3}$, and the initial position and orientation were

$$\begin{aligned}\boldsymbol{\eta}_S&=\begin{bmatrix}1 & 1 & 0.1\end{bmatrix}^{\mathrm{T}}\\ \boldsymbol{v}_S&=\begin{bmatrix}0 & 0 & 0\end{bmatrix}^{\mathrm{T}}\end{aligned}\tag{54}$$

From this table, it can be seen that the position and orientation accuracies are all acceptable, and the energy consumptions of each LGR points have no significant differences. N=4 was selected because its computation time is short enough for practical application.

Table 2
Comparison of different LGR points

LGR points	4	6	8	10	12
Terminal position error, m	8.024×10^{-5}	4.272×10^{-5}	1.171×10^{-5}	1.446×10^{-5}	8.626×10^{-6}
Terminal ψ error, rad	2.454×10^{-12}	1.543×10^{-14}	1.314×10^{-14}	1.508×10^{-15}	1.538×10^{-13}
Energy Consumption	5.620×10^{5}	5.565×10^{5}	5.551×10^{5}	5.545×10^{5}	5.543×10^{5}
Max computation time, s	8.855×10^{-4}	1.968×10^{-3}	3.632×10^{-3}	3.751×10^{-3}	4.615×10^{-3}
Average computation time, s	5.504×10^{-4}	8.122×10^{-4}	1.247×10^{-3}	1.815×10^{-3}	2.374×10^{-3}

5.2. Comparison with the lqr function of Matlab

A Matlab function 'lqr' was used to verify the performance of the proposed method. lqr function uses the Schur algorithm to solve the algebraic Riccati equation. It is well-known that this method is potentially unstable, numerical intensive and not efficient (Yan, Fahroo and Ross, 2001) and thus cannot be used for the dynamic positioning of USV. This method can design the optimal control for linear system and compared here to illustrate the performance of the proposed method. The comparison results of position, orientation and control inputs between the proposed method and lqr function are shown below. It can be seen that the results of the proposed method are almost the same with the results of lqr function indicating that the proposed method can get an accurate result in an optimal way. Here the environment forces and the control inputs saturation and the parameters on the diagonal position in $A(x)$ are not considered to make sure that the problem can be solved by using lqr function of the Matlab.

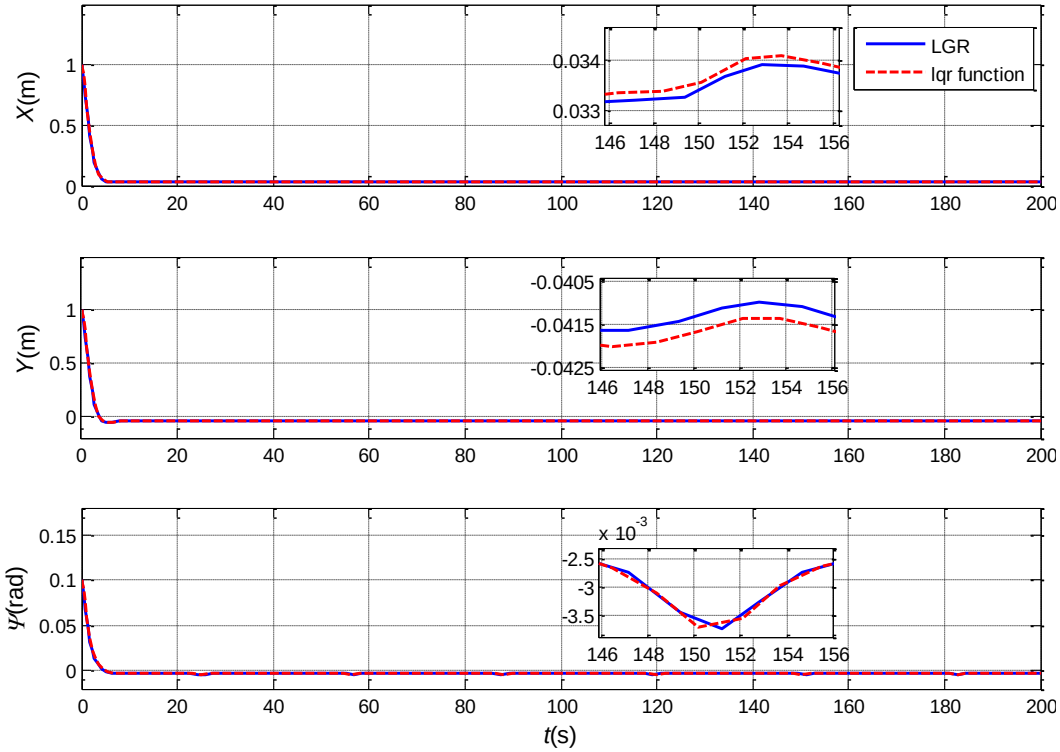

Fig. 2. Comparison of the position and orientation between the proposed method and the lqr function.

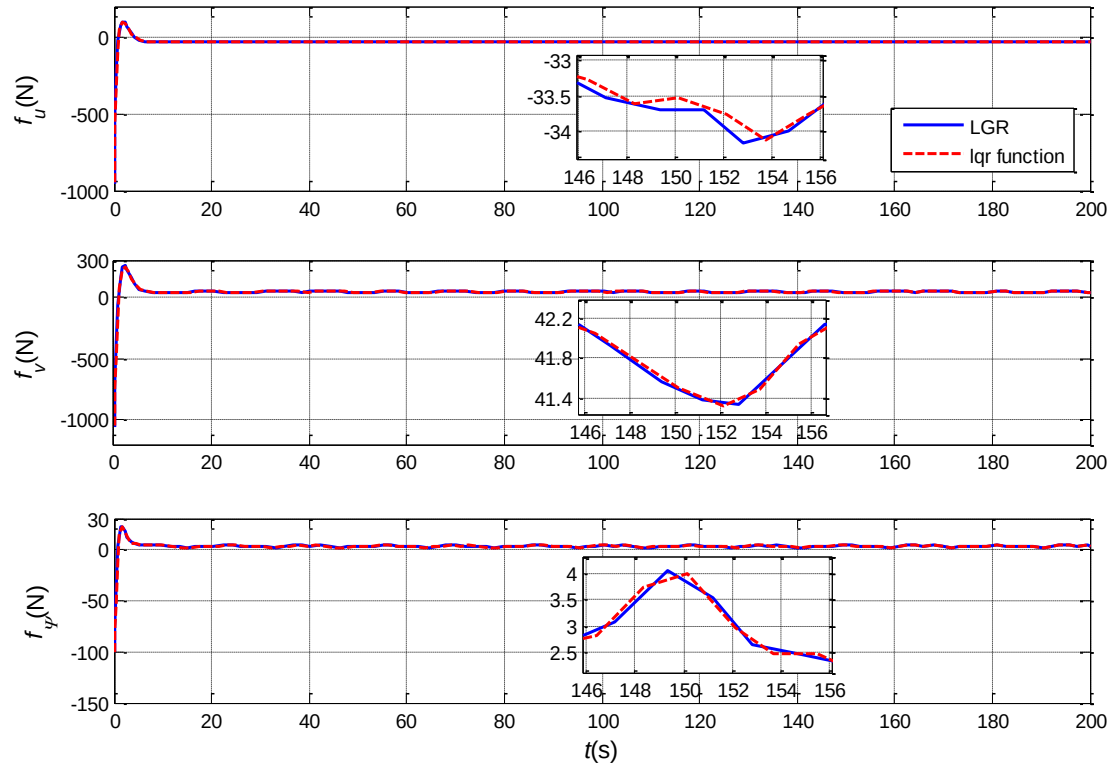

Fig. 3. Comparison of the control inputs between the proposed method and the lqr function.

5.3. Simulation results considering control input saturation

Considering a harsh working conditions of USV with the wind and current disturbances assumed as V_w=2m/s, $\gamma_w = -\pi/4$, V_c=2m/s, $\beta_c = -\pi/2$. A time variant disturbance was denoted as $d(t)$ to include all the unknown external environmental disturbances.

$$d(t) = \begin{bmatrix} 0.4\sin(0.3t) + 0.3\cos t - 1 \\ -0.15\sin(0.2)t + 0.3\cos(0.5t) + 1.5 \\ 0.3\sin t + 0.8\sin(0.4t) + 1 \end{bmatrix} \tag{55}$$

It was assumed that the max control inputs for surge, sway and yaw are all 300N. Eqn. (53) was used to solve the Eqn. (30), where

$$\bar{\boldsymbol{Q}} = \begin{bmatrix} 10^7 & & & & & & & & & \\ & 10^7 & & & & & & & 0 & \\ & & 10^7 & & & & & & & \\ & & & 10^7 & & & & & & \\ & & & & 6\times10^6 & & & & & \\ & & & & & 6\times10^6 & & & & \\ & & & & & & 2\times10^4 & & & \\ & 0 & & & & & & 2\times10^4 & & \\ & & & & & & & & 2\times10^4 & \end{bmatrix} \tag{56}$$

$$\bar{\boldsymbol{R}} = \begin{bmatrix} 10 & & \\ & 10 & \\ & & 10 \end{bmatrix} \tag{57}$$

The matrices $\bar{\boldsymbol{Q}}$ and $\bar{\boldsymbol{R}}$ were derived by trial and error method. The simulation results are shown in Fig. 4-6. Table 3 shows some details of this simulation. From these results, it can be seen that the computational time and the errors are all acceptable within limits for real application and the control inputs are also not saturated in the entire process.

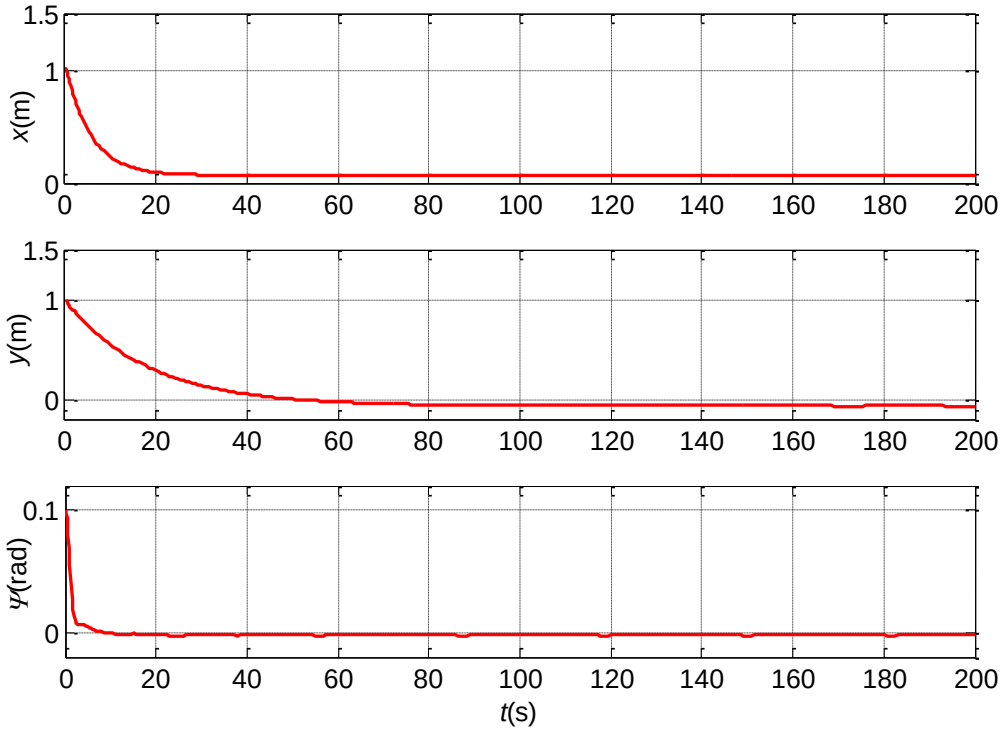

Fig. 4. Positions and orientation of USV.

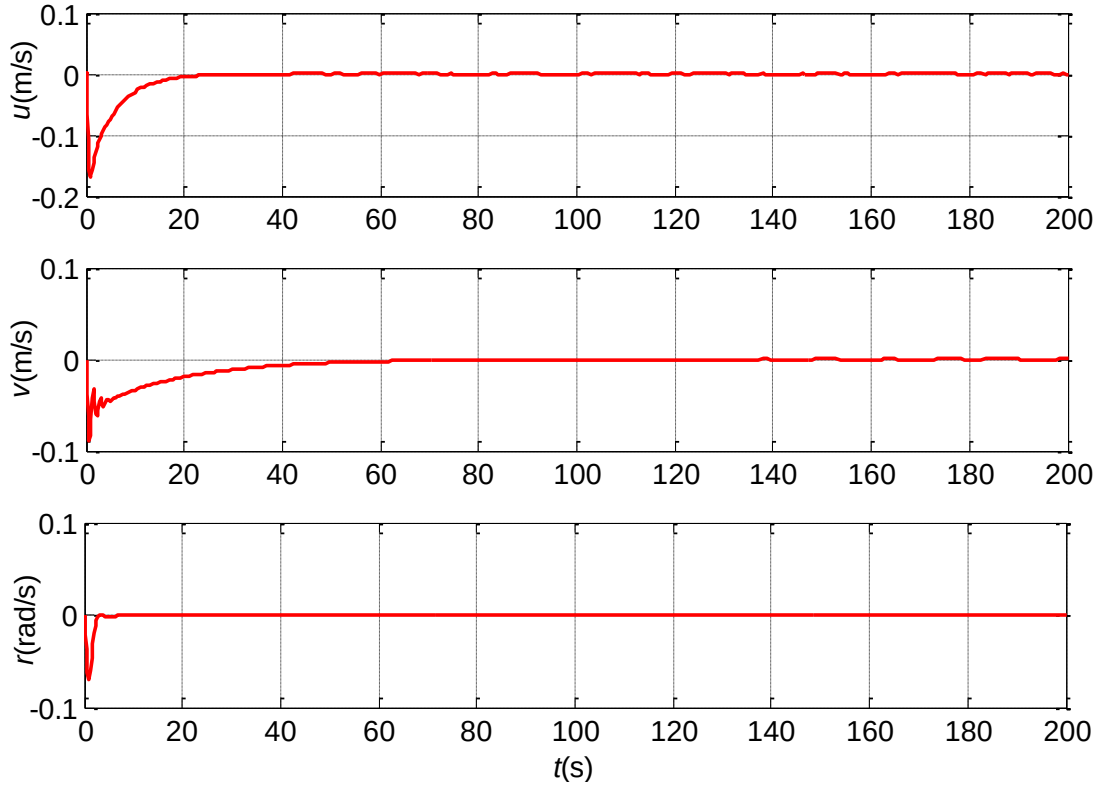

Fig. 5. Velocities and angle velocity of USV.

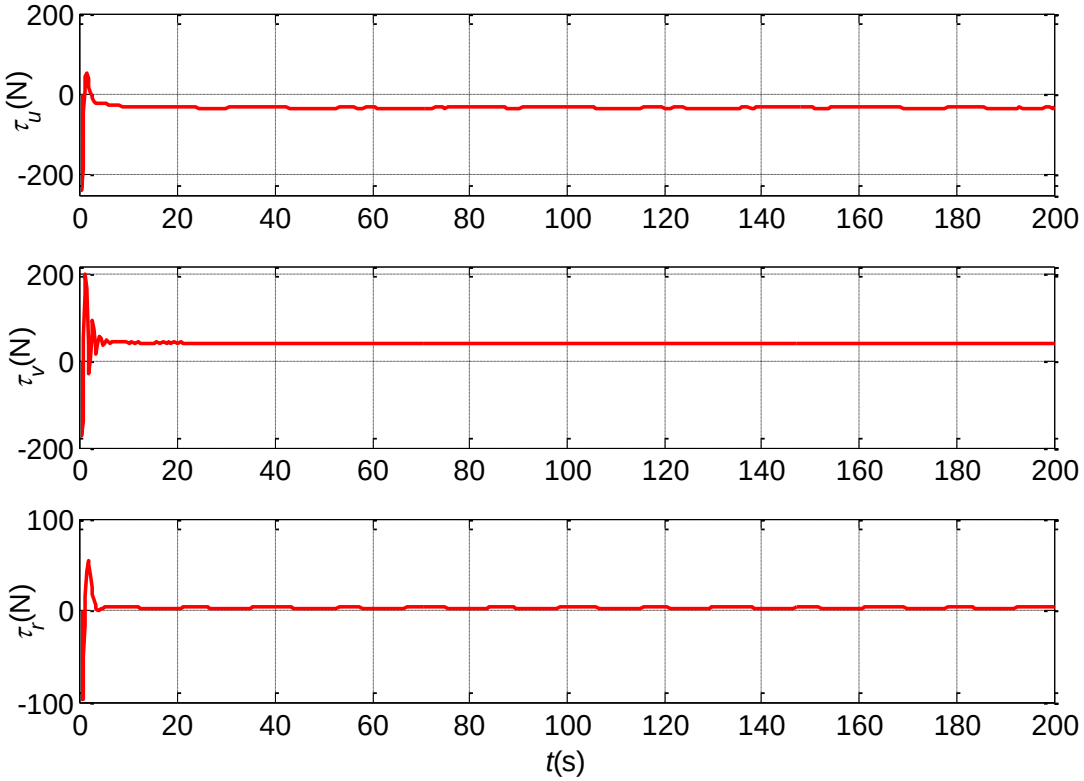

Fig. 6. Control inputs of the USV.

Table 3
Computation results considering control input saturation

Terminal x error, m	0.067	Terminal u error, m/s	8.519×10^{-5}
Terminal y error, m	-0.066	Terminal v error, m/s	2.760×10^{-5}
Terminal ψ error, rad	-0.002	Terminal r error, rad/s	1.100×10^{-4}
Energy consumption	6.347×10^{5}	Average computation time, s	4.928×10^{-3}

5.4. Simulation results with a big initial error

A bigger initial error was given to test the performance of the proposed method. The initial position and orientation were

$$\boldsymbol{\eta}_S = [10 \quad 10 \quad 1]^{\mathrm{T}} \tag{58}$$

which was 10 times of the last section.

The results of position and orientation, velocities and angle velocity and the control inputs are shown in Figs. 7-9. It can be seen that the control inputs are a nearly bang-bang control in the first 30 seconds, because the initial error is very big. The system then converge to the balance point under the disturbance. The terminal errors, energy consumption and computation time are shown in table 4. From the table, it can be seen that the errors and computation time are almost the same with the results in the last section, which shows the good performance of the proposed method with different

initial errors.

For this big error, proper $\boldsymbol{Q}$ and $\boldsymbol{R}$ could not be found to make the system stable without using the control input saturation technique. Whilst the $\bar{\boldsymbol{Q}}$ and $\bar{\boldsymbol{R}}$ are the same for section 5.3 and 5.4 which means the proposed method is robust for any proper initial error.

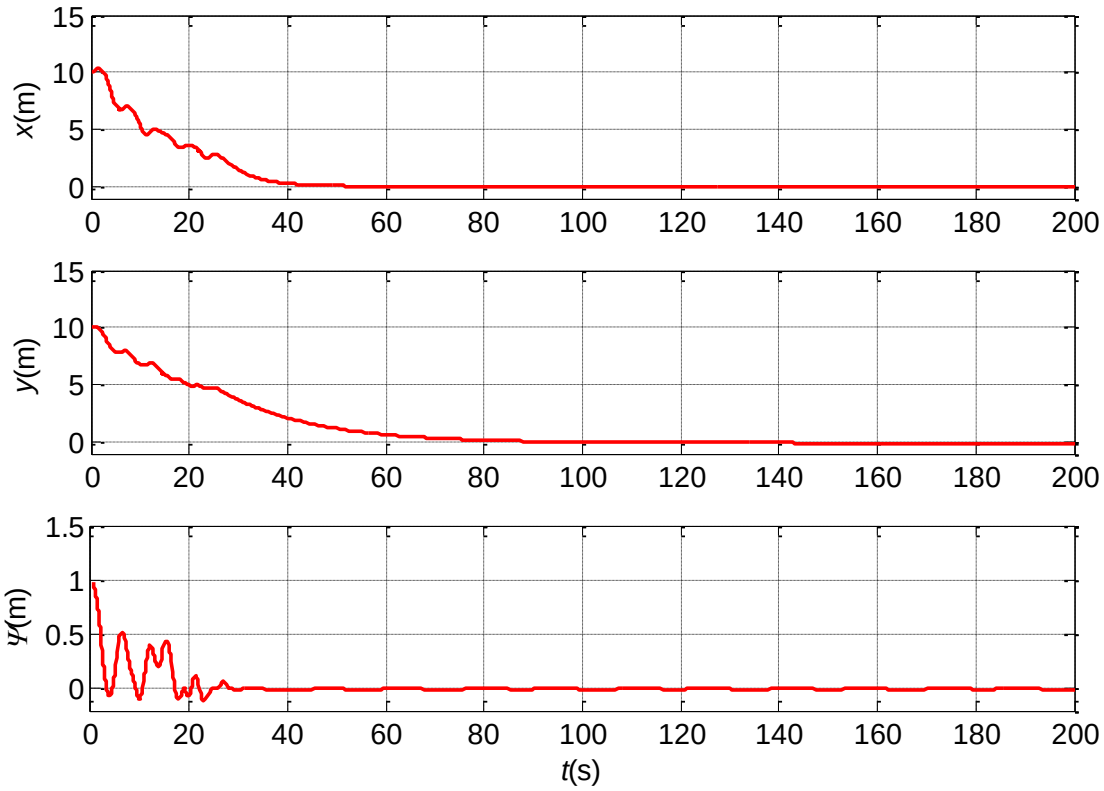

Fig. 7. Positions and orientation for a big initial error example.

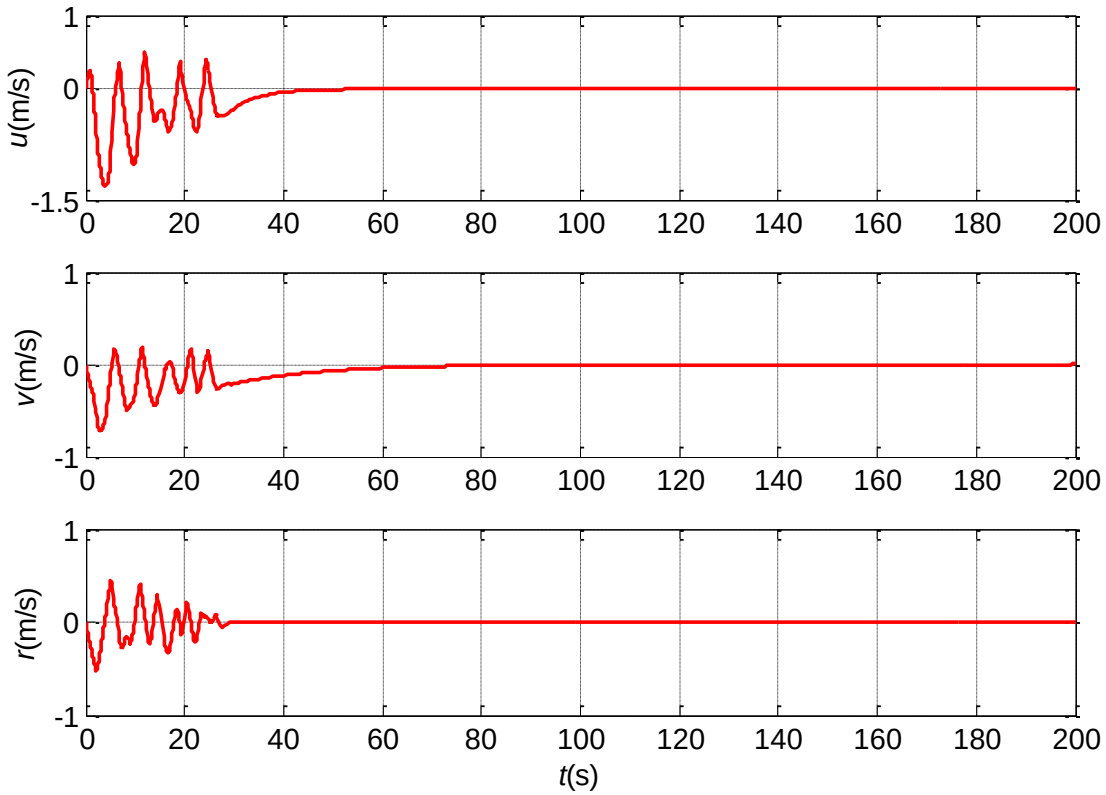

Fig. 8. Velocities and angle velocity for a big initial error example

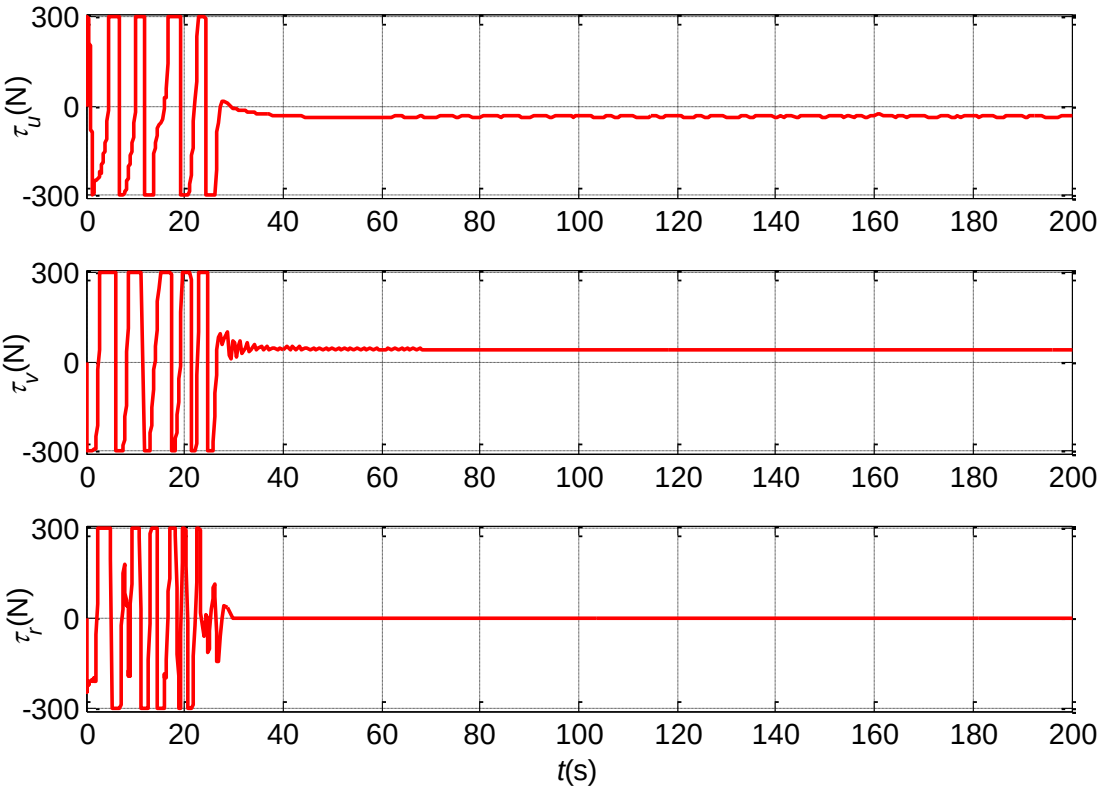

Fig. 9. Control inputs for a big initial error example.

Table 4
Computation results considering control input saturation for a big initial error example

Terminal x error, m	0.068	Terminal u error, m/s	-4.428×10^{-5}
Terminal y error, m	-0.066	Terminal v error, m/s	9.974×10^{-6}
Terminal ψ error, rad	-0.002	Terminal r error, rad/s	1.100×10^{-4}
Energy Consumption	5.722×10^{6}	Average computation time, s	4.796×10^{-3}

6. Conclusions

A novel dynamic positioning method for an USV has been proposed in this paper. A state-dependent Riccati equation (SDRE) technique is used to solve the dynamic positioning problem. Then an extended state-dependent coefficient (SDC) is used to consider the control inputs saturation for practical application. A Legendre-Gauss-Radau pseudospectral method is introduced to avoid solving complex algebraic Riccati equation so that calculation for SDRE can be performed in real-time. Simulation results show the accuracy of the proposed method compared with the lqr function of Matlab, and illustrates the excellent performance of the proposed methodology in real-time.

The dynamic position may be required to be achieved in a finite time horizon for practical applications and the problem will not be an ITHNOC problem but will become a finite time horizon nonlinear optimal control (FTHNOC) problem. State-Dependent Differential Riccati Equation (SDDRE) technique which is developed from SDRE, is designed to deal with the FTHNOC problem. SDDRE needs to solve differential Riccati equation and is more difficult to solve compare to SDRE. The efficient solution for SDDRE will be studied in future.

Acknowledgments

This work was supported in part by the Fundamental Research Funds for the Central Universities under Grant nos. HIT.NSRIF.2013135 and HIT.KISTP.2014029, the Natural Scientific Research Innovation Foundation in Harbin Institute of Technology under Grant no. HIT.NSRIF.2014139, the Science and Technology Foundation for the Universities in Shandong Province under Grant no. J14LN93.

The authors thank for the financial support from China Scholarship Council.

Reference:

Çimen Tayfun. Survey of State-Dependent Riccati Equation in Nonlinear Optimal Feedback Control Synthesis. Journal of Guidance, Control and Dynamics, 35(4): 1025-1047, 2012.

Çimen Tayfun. Systematic and effective design of nonlinear feedback controllers via the state-dependent Riccati equation (SDRE) method. Annual Reviews in Control, 34: 32-51, 2010.

Cloutier James R. State-dependent Riccati equation techniques: an overview. Proceedings of the American Control Conference, New Mexico, June, 1997, 932-936.

Donaire Alejandro and Perez Tristan. Dynamic Positioning of Marine Craft Using a Port-Hamiltonian Framework. Automatica, 48: 851-856, 2012.

Du Jialu, Yang Yang, Wang Dianhui, Guo Chen. A Robust Adaptive Neural Networks Controller for Maritime Dynamic Positioning System. Neurocomputing, 110: 128-136, 2013.

Fahroo Fariba and Ross I. Michael. Pseudospectral methods for infinite-horizon nonlinear optimal control problems. Journal of Guidance, Control and Dynamics, 31(4): 927-936, 2008.

Fossen Thor. I. Guidance and Control of Ocean Vehicles. UK: John Wiley & Sons Ltd., 1994.

Fossen Thor I. and Grøvlen Aslaug. Nonlinear Output Feedback Control of Dynamically Positioned Ships Using Vectorial Observer Backstepping. IEEE Transactions on Control Systems Technology, 6(1): 121-128, 1998.

Garg Divya, Hager William W. and Rao Anil V.. Pseudospectral methods for solving infinite-horizon optimal control problems. Automatica, 47: 829 – 837, 2011.

Katebi M.R., Grimble M.J. and Zhang Y. H∞ Robust Control Design for Dynamic Ship Positioning. IEE Proceedings on Control Theory and Applications, 110-120, 1997.

Loria Antonio, Fossen Thor I. and Panteley Elena. A Separation Principle for Dynamic Positioning of Ships: Theoretical and Experimental Results. IEEE Transactions on Control Systems Technology, 8(2): 332-343, 2000.

Mracek Curtis P. and Cloutier James R. Control designs for the nonlinear benchmark problem via the state-dependent Riccati equation method. International Journal of Robust and Nonlinear Control, 8: 401-433, 1998.

Muhammad S. and Doria-Cerezo A.. Passivity-based Control Applied to the Dynamic Positioning of Ships, IET Control Theory and Applications, 6(5): 680-688, 2012.

Nguyen Trong Dong, Sørensen Asgeir J. and Quek Ser Tong. Design of Hybrid Controller for Dynamic Positioning from Calm to Extreme Sea Conditions. Automatica 43: 768-785, 2007.

Panagou Dimitra and Kyriakopoulos Kostas J.. Dynamic Positioning for an

Underactuated Marine Vehicle Using Hybrid Control. International Journal of Control, 87(2): 264-280, 2014.

Pettersen Kristin Y. and Fossen Thor I.. Underactuated Dynamic Positioning of a Ship-Experimental Results. IEEE Transactions on Control Systems Technology, 8(5): 856-863, 2000.

Pereira Arvind, Das Jnaneshwar and Sukhatme Gaurav S. An Experimental Study of Station Keeping on an Underactuated ASV. IEEE/RSJ International Conference on Intelligent Robots and Systems, France, 3164-3171, 2008.

Sørensen Asgeir J.. A Survey of Dynamic Positioning Control Systems. Annual Reviews in Control, 35: 123-136, 2011.

Sørensen A. J., Sagatun S. I. and Fossen T. I. Design of A Dyanmic Positioning System Using Model-based Control. Control Engineering Practical, 4(3): 359-368, 1996.

Tannuri E.A., Agostinho A.C., Morishita H.M. and Moratelli Jr L. Dynamic Positioning Systems: An Experimental Analysis of Sliding Mode Control. Control Engineering Practice, 18: 1121-1132, 2010.

Yan Hui, Fahroo Fariba and Ross I. Michael. Optimal feedback control laws by Legendre pseudospectral approximations. Proceedings of the American Control Conference, Arlington, VA June, 2001, 2388-2393.